Progress in Fractional Differentiation and Applications
An International Journal

http://dx.doi.org/10.18576/pfda/110408

Consistent Numerical Scheme and Unique Existence of the Solutions for Fractional COVID-19 Model

Mohamed A. Hafez [1,2], *Montasir Qasymeh* [3], *Ali Akgül* [4,5,*], *Zafar Iqbal* [6], *Nauman Ahmed* [6], *Muhammad Shahzad*[6], *and Betty Wan Voon* [7]

[1] Faculty of Engineering and Quantity Surviving, INTI International University Colleges, Nilai, Malaysia
[2] Faculty of Management, Shinawatra University, Pathum Thani, Thailand
[3] Electrical and Computer Engineering Department, Abu Dhabi University, Abu Dhabi, United Arab Emirates
[4] Department of Electronics and Communication Engineering, Saveetha School of Engineering, SIMATS, Chennai, Tamilnadu, India
[5] Department of Mathematics, Art and Science Faculty, Siirt University, 56100 Siirt, Turkey
[6] Department of Mathematics and Statistics, The University of Lahore, Lahore, Pakistan
[7] Department of Civil Engineering, (COE), Universiti Tenaga Nasional, Kajang, Malaysia

Received: 11 Aug. 2024, Revised: 17 Sept. 2024, Accepted: 20 Oct. 2024
Published online: 1 Oct. 2025

Abstract: This study discusses coronavirus disease) coronavirus with mathematical approaches. Coronavirus disease 2019 (COVID-19) is a pandemic breathing problem that spreads from person-to-others caused by a coronavirus and poses a serious public health risk. The goal of this research is to apply a modified susceptible, exposed, infectious, recovered (SEIQR) compartmental mathematical model to predict the COVID-19 epidemic dynamics model. Another research achievement is to define a modified SEIQR model of coronavirus disease 2019 (COVID-19) with fractional order using the Caputo derivative. We analyze the result as existence and uniqueness using fixed-point theory, global and local stability at DFE and EE, Reproductive number, and explore the GL-NSFD Scheme for the proposed model. Moreover, we evaluated positivity and boundedness in the GL-NSFD Scheme in general. Moreover, shows the behavior of the results from the fractional differential equation in different ways by plotting the figures at the bottom of the article, and then describes the final analysis of the model.

Keywords: Covid-19; fractional derivative; Lipschitz condition; self-mapping; contraction; stability; numerical simulation.

1 Introduction

The coronavirus, named COVID-19 by the World Health Organization (WHO) on the eleventh of February 2020 is in charge of the present spread of pneumonia, which was found in the first week of December 2019, close to the city of Wuhoan in Hubei province, China [1]. COVID-19 can also cause the disease. Coronaviruses are essentially the cause of respiratory and gastrointestinal tract infections. Generally, Coronaviruses are distributed into four main types: Alpha, Beta, Gamma, and Delta-Coronavirus, where Gamma-Coronavirus and Delta-Coronavirus mostly infect birds, While the Beta-Coronavirus and Alpha-Coronavirus mainly infect mammals [2].

Recently, the rate of deaths around the sector has increased dramatically because of the spreading of the brand's latest virus, referred to as the coronavirus (COVID-19) [3]. The rapid increase in instances has generated an actual assignment internationally, particularly when the World Health Organization (WHO) announced that this virus has ended up a worldwide pandemic given that its outbreak has unfolded unbelievably from China to the relaxation of the sector. Most nations around the sector have applied techniques primarily based completely on limiting movement or journeying to decrease the spreading of the probably lethal virus among nations [4]. Despite the dangerous effect of reaching economic growth, confined movement is considered one of the best ways to lessen the virus [5].

The new SARS-COV-2 is known as severe acute respiratory syndrome coronavirus, which gives rise to the COVID-19 epidemic. This latest pathogen has spread very quickly, exceeding 200 states. Since COVID-19 killed over 9,391 people in March 2020 the infected persons cases of 2,023,082 approximately exceeding 180 different states [6]. Moreover, according

* Corresponding author e-mail: aliakgul00727@mail.com

to information from the World Health Organization (WHO) that all over the world, as of 2:00 am central European summer time (CEST), 27th of the fourth month in 2020, there were 2,858,635 infected cases of COVID-19, incorporating 1,96,295 expired in exceeding hundred and thirteen countries. Globally, almost five hundred and thirty-one million people have been affected by COVID-19 [7].

In the next few days, the slow percentage of affected individuals increases [8]. The percentage of recovered people has also increased. Almost five hundred and two million people have recovered from this dangerous disease. Moreover, there is no special treatment, no special medicine, or proper vaccine to cure infected patients completely; there is an increase in the number of deaths of deceased people step-by-step [9]. For more clarity, the worth and economy of every affected country is decreasing day by day due to the infection rate of this dangerous virus [10].

Initially, every infected individual experienced a big-stage fever, faculty in cough, and shortness in breath, retransmitted by touching the body or hand-shaking the infected person to the uninfected people from their eyes, nose, mouth, and other organs of their bodies. For control, the spread of this dangerous virus, every state is ready to take almost all fundamental and public concerns for health are due to this happenings paid all over the world on how many persons are infected by this epidemic and how many persons are suspected to have this disease to prevent or avoid its sudden effects on humankind.

Since the beginning of the outbreak in Wuhan, many modeling classes worldwide have reported statistics and future predictions for the COVID-19 epidemic in journal publications and online websites (see [11]). Mathematical methods play an increasing number of critical roles in our mathematical expertise in the transmission and management of epidemic diseases [12]. The mathematical models related to epidemiological studies are established in consisting of proposing, future planning, further implementing, testing studies, controlling, and computing a number of detection, therapy, and control programs. In addition, to examine, analyze, study, test, there is a big difference between the prediction and actual when it comes to reality could be due to the occurrence of unexpected factors [13], which could not be predicted by using the historical statistic.

To search for and cure these types of diseases properly, we require an effective technique to evaluate these mathematical models. To evaluate the linear and nonlinear systems of differential equations (DE), many techniques exist, such as the exact solution method, approximate solution method, and special numerical and stochastic systems. Most of these mathematical systems are computationally expensive or require complicated computations by samples [14]. Normally, the exact types of system solutions are very difficult and complicated [15]-[24].

2 Preliminaries

This section presents fundamental definitions, important results, and key theorems from fixed-point theory relevant to our research.

Definition 2.1 Caputo fractional order derivative

$$ {}_0^cD_t^{\nu} s(t) = \frac{1}{\Gamma(1-\nu)} \int_0^t \frac{s'(\tau)}{(t-\tau)^{\nu}} d\tau, \quad 0 < \nu \leq 1, \quad t > 0 \tag{1} $$

And the corresponding inversion defined by:

$$ {}_0^cI_t^{\nu} s(t) = \frac{1}{\Gamma(\nu)} \int_0^t \frac{s(\tau)}{(t-\tau)^{1-\nu}} d\tau, \quad 0 < \nu \leq 1, \quad t > 0 \tag{2} $$

Definition 2.2 In a function, a fixed or invariant point is a value of the independent variable that does not change in a given transformation. Mathematically, In a function $s(t)$, a point t_0 is a fixed point if and only if:

$s(t_0) = t_0$.

Theorem 2.3 Let B be a convex, closed, and non-empty set in T_2 topological space. If $\hbar$, R are continuous self-mappings such that:

$\hbar : t \to t, \quad R : t \to t$

in a subset of compact set B, then R has a fixed point.

Theorem 2.4 Let (X,d) be a metric space and $s : t \to t$ be a self-mapping such that:

$d[s(t_1), s(t_2)] \leq kd[t_1, t_2]$

for some $0 \leq k < 1$ and $\forall t_1, t_2 \in t$. Then s is a contraction mapping and has a unique fixed point in t.

3 Model Extension

Mathematical models are helpful tools for recognizing the conduct of infection when they become harmful to society. To analyze this type of transmission we need some authentic mathematical tools which few of them are different equations, initial conditions, working parameters, and statistical estimation.

3.1 COVID-19 Model

This subsection of the article consists of fundamental information about the time-dependent system of five ordinary differential equations, a mathematical SEIQR model for the COVID-19 virus with their necessary parameters and variables:

$$\frac{dS(t)}{dt} = \Lambda - \mu S(t) - \beta(N)S(t)(E(t)+I(t)) \tag{3}$$
$$\frac{dE(t)}{dt} = \beta(N)S(t)(E(t)+I(t)) - \pi E(t) - (\mu+\gamma)E(t) \tag{4}$$
$$\frac{dI(t)}{dt} = \pi E(t) - \sigma I(t) - \mu I(t) \tag{5}$$
$$\frac{dQ(t)}{dt} = \gamma E(t) + \sigma I(t) - \theta Q(t) - \mu Q(t) \tag{6}$$
$$\frac{dR(t)}{dt} = \theta Q(t) - \mu R(t) \tag{7}$$

Variables and Parameter Descriptions

Symbol	Description
S	Susceptible Individuals
E	Exposed Persons
I	Infected Persons
Q	Isolated People
R	Recovered People
β	Rate at which Susceptible Persons move to Infected and Exposed Population
π	Rate at which Exposed People move to Infected class
γ	Rate at which Exposed class becomes isolated
σ	Rate at which Infected class is added to isolated individuals
θ	Rate at which isolated persons recover
μ	Rate of natural deaths and deaths by disease

The underlying informative first four equations are free from $R(t)$, therefor we omit without generality the 5th equation for $R(t)$ and we modified the above system of equations as fallows,

$$\frac{dS(t)}{dt} = \Lambda - \mu S(t) - \beta(N)S(t)(E(t)+I(t)),$$
$$\frac{dE(t)}{dt} = \beta(N)S(t)(E(t)+I(t)) - \pi E(t) - (\mu+\gamma)E(t),$$
$$\frac{dI(t)}{dt} = \pi E(t) - \sigma I(t) - \mu I(t),$$
$$\frac{dQ(t)}{dt} = \gamma E(t) + \sigma I(t) - \theta Q(t) - \mu Q(t).$$

For this new modified system of equations we suppose $N = \Lambda/\mu$, $s = S/N$, $e = E/N$, $i = I/N$, and $q = Q/N$, and we attain the normalized form of COVID-19 model with system of four time-dependent ordinary differential equations as

follows,

$$\frac{ds}{dt} = \mu - \mu s - \beta N s(e+i), \tag{8}$$
$$\frac{de}{dt} = \beta N s(e+i) - \pi e - (\mu+\gamma)e, \tag{9}$$
$$\frac{di}{dt} = \pi e - \sigma i - \mu i, \tag{10}$$
$$\frac{dq}{dt} = \gamma e + \sigma i - \theta q - \mu q. \tag{11}$$

The corresponding time-fractional version of the above discussed disease in four fractional differential equations (FDEs)is given by

$${}_0^cD_t^{\nu} s(t) = \mu - \mu s - \beta N s(e+i), \tag{12}$$
$${}_0^cD_t^{\nu} e(t) = \beta N s(e+i) - \pi e - (\mu+\gamma)e, \tag{13}$$
$${}_0^cD_t^{\nu} i(t) = \pi e - \sigma i - \mu i, \tag{14}$$
$${}_0^cD_t^{\nu} q(t) = \gamma e + \sigma i - \theta q - \mu q. \tag{15}$$

Subject to the below given initial value conditions at initial time $t = 0$.

$$s(0) = s_0 \geq 0, \quad e(0) = e_0 \geq 0, \quad i(0) = i_0 \geq 0, \quad q(0) = q_0 \geq 0.$$

4 Transformation of the system in fixed point operators

In this section, we want to calculate the fixed point operators of the underline important COVID-19 time fractional system (12)-(15) of nonlinear partial differential equations using different approaches in the discussion. In this system of equations we have $t > 0$ and $0 < \nu \leq 1$ with initial value conditions $s(0) = s_0 \geq 0$, $e(0) = e_0 \geq 0$, $i(0) = i_0 \geq 0$, $q(0) = q_0 \geq 0$.

In this article, we shall use definition of Caputo type fractional order derivative (1) and the inverse derivative (2), the above underlying system (12)-(15) convert into the following Volterra type integral equations:

$$G_s(t) = s_0 + \frac{1}{\Gamma(\nu)} \int_0^t \frac{\mu - \mu s - \beta N s(e+i)}{(t-\tau)^{1-\nu}} d\tau, \tag{16}$$
$$G_e(t) = e_0 + \frac{1}{\Gamma(\nu)} \int_0^t \frac{\beta N s(e+i) - \pi e - (\mu+\gamma)e}{(t-\tau)^{1-\nu}} d\tau, \tag{17}$$
$$G_i(t) = i_0 + \frac{1}{\Gamma(\nu)} \int_0^t \frac{\pi e - \sigma i - \mu i}{(t-\tau)^{1-\nu}} d\tau, \tag{18}$$
$$G_q(t) = q_0 + \frac{1}{\Gamma(\nu)} \int_0^t \frac{\gamma e + \sigma i - \theta q - \mu q}{(t-\tau)^{1-\nu}} d\tau. \tag{19}$$

These Volterra type of first-kind integral equations (16)-(19) are called fixed point operators or in other words, known as invariant point operators for the time-fractional system of a differential equation (12)-(15) respectively.

Now, we shall proceed with the existence and uniqueness of the solutions of the COVID-19 model by using the approaches from the study of fixed point theory, such as the contraction mapping principle with Lipschitz condition, compactness with Schauder fixed-point theorem, and self-mapping as the Banach fixed-point theorem [25,26]. For evaluation, it is very important to calculate the necessary condition of self-mapping for a particular operator from (16)-(19).

5 Unique Existence

In this section, we want to extract the self-mapping, relative compactness, and contraction mapping conditions for the existence and uniqueness of the roots for mentioned time-fractional differential equations (12)-(15) by applying all the

methods discussed in the last of the section 4, for this purpose of derivation we need to some suppositions from (12)-(15) as follow,

$$H_1(t,s,e,i,q) = \mu - \mu s - \beta N s(e+i), \quad \forall t \geq 0 \tag{20}$$
$$H_2(t,s,e,i,q) = \beta N s(e+i) - \pi e - (\mu+\gamma)e, \quad \forall t \geq 0, \tag{21}$$
$$H_3(t,s,e,i,q) = \pi e - \sigma i - \mu i, \quad \forall t \geq 0, \tag{22}$$
$$H_4(t,s,e,i,q) = \gamma e + \sigma i - \theta q - \mu q. \quad \forall t \geq 0. \tag{23}$$

Consider the Caputo fractional integral fixed point operators (16)-(19) for further procedure to calculation of the conditions [27].

$$G_s(t) = s_0 + \frac{1}{\Gamma(\nu)} \int_0^t \frac{H_1(t,s,e,i,q)}{(t-\tau)^{1-\nu}} d\tau, \tag{24}$$
$$G_e(t) = e_0 + \frac{1}{\Gamma(\nu)} \int_0^t \frac{H_2(t,s,e,i,q)}{(t-\tau)^{1-\nu}} d\tau, \tag{25}$$
$$G_i(t) = i_0 + \frac{1}{\Gamma(\nu)} \int_0^t \frac{H_3(t,s,e,i,q)}{(t-\tau)^{1-\nu}} d\tau, \tag{26}$$
$$G_q(t) = q_0 + \frac{1}{\Gamma(\nu)} \int_0^t \frac{H_4(t,s,e,i,q)}{(t-\tau)^{1-\nu}} d\tau. \tag{27}$$

Suppose that C be the space of all continuous functions in the Banach space and we consider four closed balls with radius r and center s_0, e_0, i_0, q_0 respectively [28], such that

$$B_r(s_0) = \{s, s \in C[0,\rho] : \|s - s_0\| \leq r\}, \|s\| \leq (r + s_0) \quad \because s_0 > 0, \tag{28}$$
$$B_r(e_0) = \{e, e \in C[0,\rho] : \|e - e_0\| \leq r\}, \|e\| \leq (r + e_0) \quad \because e_0 > 0. \tag{29}$$
$$B_r(i_0) = \{i, i \in C[0,\rho] : \|i - i_0\| \leq r\}, \|i\| \leq (r + i_0) \quad \because i_0 > 0, \tag{30}$$
$$B_r(q_0) = \{q, q \in C[0,\rho] : \|q - q_0\| \leq r\}, \|q\| \leq (r + q_0) \quad \because q_0 > 0. \tag{31}$$

All these closed balls are helpful in imagining some fundamental necessary calculations for each of the equations and also proved helpful for the procedure to deduce the fixed-point existence and uniqueness conditions.

5.1 Construction of self-mapping

This subsection of section 4 gives us full detail about the necessary time condition of self-mapping of the system of a fractional differential equation (FDEs). First, we take the equation (24) then apply the norm on both sides of the fixed point operators and proceed the particularly evaluate the condition of self-mapping, relative compactness, and contraction mapping according to Banach fixed point theorem and Schauder fixed point theorem [31] for the solutions of (12) as follow

$$\|G_s(t) - s_0\| \leq \left| \frac{1}{\Gamma(\nu)} \right| \int_0^t \frac{\|H_1\|}{|t-\tau|^{1-\nu}} d\tau. \tag{32}$$

Consider equation (20) with norm of both sides of (20) and use (28)-(31), after some normal calculations and simplification we have,

$$\|H_1\| \leq |\mu| - |\mu|(r+s_0) - |\beta|\|N\|(r+s_0)[(r+e_0) + (r+i_0)],$$

Suppose $\|N\| \leq p$ that let $s_0 = \varpi_1$, $e_0 = \varpi_2$, $i_0 = \varpi_3$, $q_0 = \varpi_4$ and $\varpi = \max\{\varpi_1, \varpi_2, \varpi_3, \varpi_4\}$. After using these supposition we attain,

$$\|H_1\| \leq |\mu| - (r+\varpi)[|\mu| - 2|\beta|p(r+\varpi)] = H_1^*. \quad \text{(say)}$$

Now equation (32) become as,

$$\|G_s(t) - s_0\| \leq \left| \frac{1}{\Gamma(\nu)} \right| \int_0^t \frac{H_1^*}{|t-\tau|^{1-\nu}} d\tau. \tag{33}$$

Both the important cases $(t-\tau)>0$ and $(t-\tau)<0$ implies $t>\tau$, $\tau>t$ respectively, The calculation of this indefinite integral for both these described cases are necessarily attain the same result,

$$\int_0^t \frac{1}{|t-\tau|^{1-\nu}} d\tau = \frac{\rho^\nu}{\nu}.$$

This calculation of the indefinite integral have ρ is just the notation of time period length from 0 to t for each of the equation particularly. so the equation (33) become as,

$$\|G_s(t)-s_0\| \leq \left|\frac{1}{\Gamma(\nu)}\right| H_1^* \frac{\rho^\nu}{\nu}.$$

Now for the theory of self-mapping analysis, we are fully aware of the situation that the difference from the function value with the center of the ball must be less than the radius of the given closed ball in the space C of all continuous functions in Banach space so that,

$$\left|\frac{1}{\Gamma(\nu)}\right| H_1^* \frac{\rho^\nu}{\nu} \leq r.$$

Just short Simplifications for the deduction of maximum and minimum boundary for the range of the value of ρ gives,

$$\rho \leq \left[\frac{r|\Gamma(\nu)|\nu}{H_1^*}\right]^{1/\nu}.$$

For the representation of a susceptible variable, we rewrite in the most understandable form as follows,

$$\rho_s \leq \left[\frac{r|\Gamma(\nu)|\nu}{H_1^*}\right]^{1/\nu}. \tag{34}$$

Which is finally the condition of self mapping of the first equation (12) indicate the susceptible in the system of the fractional order differential equation (FDEs) of COVID-19 disease. And similarly we deduce the other condition for the value range of ρ we have,

$$\rho_e \leq \left[\frac{r|\Gamma(\nu)|\nu}{H_2^*}\right]^{1/\nu}, \quad \because H_2^* = \{2|\beta|p(r+\varpi)-|\pi|-(|\mu|+|\gamma|)\}(r+\varpi)\}. \tag{35}$$

$$\rho_i \leq \left[\frac{r|\Gamma(\nu)|\nu}{H_3^*}\right]^{1/\nu}, \quad \because H_3^* = \{|\pi|-p-\mu\}(r+\varpi)\}. \tag{36}$$

$$\rho_q \leq \left[\frac{r|\Gamma(\nu)|\nu}{H_4^*}\right]^{1/\nu}, \quad \because H_4^* = \{|\gamma|+p-\theta-\mu\}(r+\varpi)\}. \tag{37}$$

Hence, we are warmly excited to completion of the self-mapping analysis and we achieved the non-equating condition (35)-(37) for ρ particularly, are the conditions of self-mapping for (13)-(15) respectively.

5.2 Compactness

This part of the analysis provides the behavior of the functions of a system of time-dependent fractional differential equations (FDEs) in the COVID-19 model. The results describe the relative compactness between the families of uniformly continuous sequences of functions [32]. In this subsection, we present an evaluation of the Schauder condition using the Arzela-Ascoli theorem for computational and statistical observations. Our study of this section gives us a clearance about the existence of at least one solution to the system. To the requirements, we suppose a family of a sequence of the images s_j, e_j, i_j, q_j for the family of the sequence of pre-images $[G_s(t)]_j, [G_e(t)]_j, [G_i(t)]_j, [G_q(t)]_j$, particularly for each of the function time-depended variable in the system of fractional differential equation of COVID-19 model.

$$[G_s(t)]_j = s_0 + \frac{1}{\Gamma(\nu)}\int_0^t \frac{H_1(t,s,e,i,q)}{(t-\tau)^{1-\nu}}d\tau, \tag{38}$$

$$[G_e(t)]_j = e_0 + \frac{1}{\Gamma(\nu)}\int_0^t \frac{H_2(t,s,e,i,q)}{(t-\tau)^{1-\nu}}d\tau, \tag{39}$$

$$[G_i(t)]_j = i_0 + \frac{1}{\Gamma(\nu)}\int_0^t \frac{H_3(t,s,e,i,q)}{(t-\tau)^{1-\nu}}d\tau, \tag{40}$$

$$[G_q(t)]_j = q_0 + \frac{1}{\Gamma(\nu)}\int_0^t \frac{H_4(t,s,e,i,q)}{(t-\tau)^{1-\nu}}d\tau. \tag{41}$$

Our aim was to describe the functions for susceptible populations and exposed groups of people, infected persons, and isolated populations as equi-continuous families of the supposed sequences for each of the equations. Therefore, to continue the further process and necessary circumstance we need to choose a fixed point $t^o \in (0,t)$ to achieve the required target.

$$[G_s(t^o)]_j = s_0 + \frac{1}{\Gamma(\nu)}\int_0^{t^o} \frac{H_1(t^o,s,e,i,q)}{(t^o-\tau)^{1-\nu}}d\tau, \tag{42}$$

$$[G_e(t^o)]_j = e_0 + \frac{1}{\Gamma(\nu)}\int_0^{t^o} \frac{H_2(t^o,s,e,i,q)}{(t^o-\tau)^{1-\nu}}d\tau, \tag{43}$$

$$[G_i(t^o)]_j = i_0 + \frac{1}{\Gamma(\nu)}\int_0^{t^o} \frac{H_3(t^o,s,e,i,q)}{(t^o-\tau)^{1-\nu}}d\tau, \tag{44}$$

$$[G_q(t^o)]_j = q_0 + \frac{1}{\Gamma(\nu)}\int_0^{t^o} \frac{H_4(t^o,s,e,i,q)}{(t^o-\tau)^{1-\nu}}d\tau. \tag{45}$$

Now subtract the equation (42) from the equation (38) and take the norm on both sides, we have

$$\|[G_s(t)]_j - [G_s(t^o)]_j\| \leq \frac{1}{|\Gamma(\nu)|}\int_0^t \frac{\|H_1(t,s,e,i,q)\|}{|t-\tau|^{1-\nu}}d\tau - \frac{1}{|\Gamma(\nu)|}\int_0^{t^o} \frac{\|H_1(t^o,s,e,i,q)\|}{|t^o-\tau|^{1-\nu}}d\tau.$$

From the equation (20) with the use of the equation (28)-(31), we have

$$\begin{aligned}\|[G_s(t)]_j - [G_s(t^o)]_j\| \leq{}& \frac{1}{|\Gamma(\nu)|}\int_0^t \frac{|\mu| - |\mu|(r+s_0) - |\beta|\|N\|(r+s_0)[(r+e_0)+(r+i_0)]}{|t-\tau|^{1-\nu}}d\tau \\ &- \frac{1}{|\Gamma(\nu)|}\int_0^{t^o} \frac{|\mu| - |\mu|(r+s_0) - |\beta|\|N\|(r+s_0)[(r+e_0)+(r+i_0)]}{|t^o-\tau|^{1-\nu}}d\tau.\end{aligned}$$

Suppose $\|N\| \leq p$ and $\varpi = \max\{\varpi_1, \varpi_2, \varpi_3, \varpi_4\}$ where $s_0 = \varpi_1$, $e_0 = \varpi_2$, $i_0 = \varpi_3$, $q_0 = \varpi_4$ we get,

$$\|[G_s(t)]_j - [G_s(t^o)]_j\| \leq \frac{1}{|\Gamma(\nu)|}\left[|\mu| - |\mu|(r+\varpi) - 2p|\beta|(r+\varpi)^2\right] \tag{46}$$

$$\times \left[\int_0^t \frac{1}{|t-\tau|^{1-\nu}}d\tau - \int_0^{t^o} \frac{1}{|t^o-\tau|^{1-\nu}}d\tau\right]. \tag{47}$$

Consider,

$$\chi = \left[\int_0^t \frac{1}{|t-\tau|^{1-\nu}}d\tau - \int_0^{t^o} \frac{1}{|t^o-\tau|^{1-\nu}}d\tau\right].$$

We observe there are two main cases necessary to solve in this calculation: the first case deals with the problem when t^o lies inside the time length interval $[0,t]$ means $t^o < t$, and the other case appears in the study when we see t inside the fixedly chosen point time-interval $[0,t^o]$ means $t^o > t$. Therefore, we calculate the integral χ for both cases, starting this evaluation with the first case of this complicated problem to approach the mean value theorem of fundamental calculus for the continuous and differentiable function within the given interval.

$$\chi = \left[\int_0^t \frac{1}{|t-\tau|^{1-\nu}}d\tau - \int_0^{t^o} \frac{1}{|t^o-\tau|^{1-\nu}}d\tau + \int_t^{t^o} \frac{1}{|t^o-\tau|^{1-\nu}}d\tau - \int_t^{t^o} \frac{1}{|t^o-\tau|^{1-\nu}}d\tau\right]$$
$$\chi = \left[\int_0^t \left\{\frac{1}{|t-\tau|^{1-\nu}} - \frac{1}{|t^o-\tau|^{1-\nu}}\right\}d\tau - \int_t^{t^o} \frac{1}{|t^o-\tau|^{1-\nu}}d\tau\right].$$

The used function inside the given integral $\Omega(t) = \frac{1}{|t-\tau|^{1-\nu}}$ is hopefully fulfill all the conditions for mean value theorem of fundamental calculus. So that, $\Omega(t) = \frac{1}{|t-\tau|^{1-\nu}}$ is a continuous function in the given time-interval $[t^o,t]$, also $\Omega(t) = \frac{1}{|t-\tau|^{1-\nu}}$ is a differentiable function on the interval $[t^o,t]$, hence there exist a fix point $\kappa \in [t^o,t]$ such that,

$$\frac{\Omega(t)-\Omega(t^o)}{t-t^o} = \Omega'(\kappa)$$
$$\frac{1}{|t-\tau|^{1-\nu}} - \frac{1}{|t^o-\tau|^{1-\nu}} \leq |t-t^o|\frac{\nu-1}{|t^o-\kappa|^{2-\nu}}$$
$$\frac{1}{|t-\tau|^{1-\nu}} - \frac{1}{|t^o-\tau|^{1-\nu}} \leq |t-t^o|\Upsilon, \quad \because \Upsilon = \frac{\nu-1}{|t^o-\kappa|^{2-\nu}}$$
$$\chi = \left[\int_0^t \{|t-t^o|\Upsilon\}d\tau - \int_t^{t^o} \frac{1}{|t^o-\tau|^{1-\nu}}d\tau\right],$$
$$\chi = \left[\{|t-t^o|\Upsilon\}t - \frac{|t^o-t|^\nu}{\nu}\right].$$

Similarly, the other case can be calculated by following the process in case-1, we will get the same result is obtained for the next case. So we have the final result of the integral as,

$$\chi = \left[\{|t-t^o|\Upsilon\}t - \frac{|t^o-t|^\nu}{\nu}\right].$$

Putting in equation (47) we get in easy form as,

$$\|[G_s(t)]_j - [G_s(t^o)]_j\| \leq \frac{1}{|\Gamma(\nu)|}\left[|\mu| - |\mu|(r+\varpi) - 2p|\beta|(r+\varpi)^2\right]\left[\Upsilon t - \frac{|t^o-t|^{\nu-1}}{\nu}\right]|t-t^o|.$$

Now! if we have the behavior of $|t-t^o|$ as $|t-t^o| \to 0$ or in other sense $t \to t^o$ then we claimed that it is mandatory in this evaluation of our observation that

$$\|[G_s(t)]_j - [G_s(t^o)]_j\| \to 0 \tag{48}$$

and if we consider the norm of the difference between t and t^o is less than δ as $|t-t^o| < \delta$ then we have the main equation in the general form as,

$$\|[G_s(t)]_j - [G_s(t^o)]_j\| \leq \Lambda\delta$$
$$\because \Lambda = \frac{1}{|\Gamma(\nu)|}\left[|\mu| - |\mu|(r+\varpi) - 2p|\beta|(r+\varpi)^2\right]\left[\Upsilon t - \frac{|t^o-t|^{\nu-1}}{\nu}\right].$$

Similarly, we generalize the results for the other remaining equations of the system of time-fractional differential equation of underlying COVID-19 model as follow:

$$\|[G_e(t)]_j - [G_e(t^o)]_j\| \leq \Delta\delta,$$
$$\because \Delta = \frac{1}{|\Gamma(\nu)|}\{2|\beta|p(r+\varpi) - |\pi| - (|\mu|+|\gamma|)\}(r+\varpi)\}\left[\Upsilon t - \frac{|t^o-t|^{\nu-1}}{\nu}\right],$$
$$\|[G_i(t)]_j - [G_i(t^o)]_j\| \leq \Theta\delta$$
$$\because \Theta = \frac{1}{|\Gamma(\nu)|}\{|\pi| - p - \mu\}(r+\varpi)\}(r+\varpi)\}\left[\Upsilon t - \frac{|t^o-t|^{\nu-1}}{\nu}\right].$$

and

$$\|[G_q(t)]_j - [G_q(t^o)]_j\| \leq \Xi\delta$$

$$\because \Xi = \frac{1}{|\Gamma(\nu)|}\{|\gamma| + p - \theta - \mu\}(r+\varpi)\}\left[\Upsilon t - \frac{|t^o - t|^{\nu-1}}{\nu}\right].$$

For $|t - t^o| > \delta$ we write

$$\|[G_s(t)]_j - [G_s(t^o)]_j\| < \varepsilon \quad \because \varepsilon = \Lambda\delta$$
$$\|[G_e(t)]_j - [G_e(t^o)]_j\| < \varepsilon \quad \because \varepsilon = \Delta\delta$$
$$\|[G_i(t)]_j - [G_i(t^o)]_j\| < \varepsilon \quad \because \varepsilon = \Theta\delta$$
$$\|[G_q(t)]_j - [G_q(t^o)]_j\| < \varepsilon \quad \because \varepsilon = \Xi\delta$$

Hence these results describe that $[G_s(t)]_j, [G_e(t)]_j, [G_i(t)]_j$ and $[G_q(t)]_j$ are equi-continuous families of the sequences of these well-known functions. Then by the use of Arzela-Ascoli theorem, we have some subsequences of these family of sequences $[G_s(t)]_{jk}, [G_e(t)]_{jk}, [G_i(t)]_{jk}, [G_q(t)]_{jk}$ for $[G_s(t)]_j, [G_e(t)]_j, [G_i(t)]_j, [G_q(t)]_j$ respectively, as $[G_s(t)]_{jk} \subseteq [G_s(t)]_j, [G_e(t)]_{jk} \subseteq [G_e(t)]_j, [G_i(t)]_{jk} \subseteq [G_i(t)]_j, [G_q(t)]_{jk} \subseteq [G_q(t)]_j$ these subsequences must be the uniformly convergent subsequences of the family of sequences. Therefore, the application of Schauder fixed point theorem investigated that $s(t), e(t), i(t), q(t)$ have surely relatively compact mapping in the family of subsequences to the family of their super-sequences of susceptible, exposed, infected and isolated population functions $s(t), e(t), i(t), q(t)$ of a system of fractional differential equations in COVID-19 model.

5.1 (Schauder fixed-point theorem) The extension of the Brouwer fixed-point theorem is called the Schauder fixed-point theorem for an infinite dimension topological space or vector space. When a convex, closed, and non-empty set ξ contain in T_2 a topological space then ϕ, φ are two different continuous mapping from ξ to itself

$$\phi = \xi - \xi, \quad \varphi = \xi - \xi$$

as $\varphi(\rho)$ contain in any subset of the compact set ξ implies φ have a mandatory fixed point.

Remark(5.2). if a sequence is proved equi-continuous than their must be the uniformly continuous and convergent subsequences $[G_s(t)]_{jk} \subseteq [G_s(t)]_j, [G_e(t)]_{jk} \subseteq [G_e(t)]_j, [G_i(t)]_{jk} \subseteq [G_i(t)]_j, [G_q(t)]_{jk} \subseteq [G_q(t)]_j$ and their are relatively compact mapping of the functions.

Remark(5.3). The relatively compactness in functions as equi-continuous of the family subsequences of their family of super-sequences in functions $s(t), e(t), i(t), q(t)$ and uniformly convergent subsequences under the self-mapping conditions (35)-(3537) are declared that there must exist at least one solution for each of the equations (12-1215) in the given space.

5.3 Origination of contraction mapping

The main theme of this section is to analyze the time-dependent condition for contraction mapping of the time-fractional differential equations of the COVID-19 model. For this purpose, we consider some assumptions regarding fixed-point operators and then proceed to calculate the Lipschitz condition. For the conversion into the Lipschitz condition of contraction mapping, we must imaginably assume two pre-images s_1, s_2, e_1, e_2, i_1, i_2 and q_1, q_2 for each of the equations in the underlying system[24] corresponding to their images $[G_s(t)]_1, [G_s(t)]_2$, $[G_e(t)]_1, [G_e(t)]_2$, $[G_i(t)]_1, [G_i(t)]_2$ and $[G_q(t)]_1, [G_q(t)]_2$ respectively. So, we describe two new a modified system of fixed point operators,

$$[G_s(t)]_1 = s_0 + \frac{1}{\Gamma(\nu)}\int_0^t \frac{H_1(t, s_1, e, i, q)}{(t-\tau)^{1-\nu}} d\tau, \tag{49}$$

$$[G_e(t)]_1 = e_0 + \frac{1}{\Gamma(\nu)}\int_0^t \frac{H_2(t, s_1, e, i, q)}{(t-\tau)^{1-\nu}} d\tau, \tag{50}$$

$$[G_i(t)]_1 = i_0 + \frac{1}{\Gamma(\nu)}\int_0^t \frac{H_3(t, s_1, e, i, q)}{(t-\tau)^{1-\nu}} d\tau, \tag{51}$$

$$[G_q(t)]_1 = q_0 + \frac{1}{\Gamma(\nu)}\int_0^t \frac{H_4(t, s_1, e, i, q)}{(t-\tau)^{1-\nu}} d\tau. \tag{52}$$

and

$$[G_s(t)]_2 = s_0 + \frac{1}{\Gamma(\nu)}\int_0^t \frac{H_1(t,s_2,e,i,q)}{(t-\tau)^{1-\nu}}d\tau, \tag{53}$$

$$[G_e(t)]_2 = e_0 + \frac{1}{\Gamma(\nu)}\int_0^t \frac{H_2(t,s_2,e,i,q)}{(t-\tau)^{1-\nu}}d\tau, \tag{54}$$

$$[G_i(t)]_2 = i_0 + \frac{1}{\Gamma(\nu)}\int_0^t \frac{H_3(t,s_2,e,i,q)}{(t-\tau)^{1-\nu}}d\tau, \tag{55}$$

$$[G_q(t)]_2 = q_0 + \frac{1}{\Gamma(\nu)}\int_0^t \frac{H_4(t,s_2,e,i,q)}{(t-\tau)^{1-\nu}}d\tau. \tag{56}$$

Subtract equation (49) form (53) and taking norm on both of the sides then simplify, we have

$$\|[G_s(t)]_1 - [G_s(t)]_2\| \leq \left|\frac{1}{\Gamma(\nu)}\right| \int_0^t \frac{\|H_1(t,s_1,e,i,q) - H_1(t,s_2,e,i,q)\|}{(t-\tau)^{1-\nu}}d\tau.$$

From equation (20), we easily calculate $H_1(t,s_1,e,i,q) - H_1(t,s_2,e,i,q)$ and get,

$$\|[G_s(t)]_1 - [G_s(t)]_2\| \leq \left|\frac{1}{\Gamma(\nu)}\right| \int_0^t \frac{[|\beta|\cdot\|N\|\cdot\|e+i\|+\mu]\cdot\|s_2-s_1\|}{(t-\tau)^{1-\nu}}d\tau.$$

Now use (28-2831) with assuming $s_0 = \varpi_1$, $e_0 = \varpi_2$, $i_0 = \varpi_3$, $q_0 = \varpi_4$ the generally say that $\varpi = \max\{\varpi_1, \varpi_2, \varpi_3, \varpi_4\}$ and suppose $\|N\| \leq p$ with short simplification we have

$$\|[G_s(t)]_1 - [G_s(t)]_2\| \leq \left|\frac{1}{\Gamma(\nu)}\right| \int_0^t \frac{[2p|\beta|(r+\varpi)+\mu]}{(t-\tau)^{1-\nu}}d\tau\|s_2-s_1\|.$$

This implies that,

$$\|[G_s(t)]_1 - [G_s(t)]_2\| \leq \left|\frac{1}{\Gamma(\nu)}\right| [2p|\beta|(r+\varpi)+\mu]\frac{\rho^\nu}{\nu}\|s_2-s_1\|.$$

As we have already awareness according to Lipschitz's condition

$$\|\Xi(\kappa_1), \Xi(\kappa_2)\| \leq \eta\|\kappa_1, \kappa_2\|$$

That is, if the norm of the difference of function value of the same function at two different points is less than or equal to the product of some constant with the norm of the difference of these points, then the mapping on that function is a contraction mapping if the such constant is less than or equal than 1 as $\eta \leq 1$. So, in our case we observe that the constant

$$\left|\frac{1}{\Gamma(\nu)}\right| [2p|\beta|(r+\varpi)+\mu]\frac{\rho^\nu}{\nu} = \eta \leq 1$$

Hence,

$$\rho \leq \left[\frac{\nu|\Gamma(\nu)|}{[2p|\beta|(r+\varpi)+\mu]}\right]^{1/\nu}$$

In the other sense, we can rewrite this equation in the form of a representation of susceptible time depended on variable $s(t)$ by representing the ρ as ρ_s.

$$\rho_s \leq \left[\frac{\nu|\Gamma(\nu)|}{[2p|\beta|(r+\varpi)+\mu]}\right]^{1/\nu}. \tag{57}$$

Which is a condition on the length of the time, where the mapping on the function of susceptible papulation depended on time $s(t)$ must be the contraction mapping. Therefore, this condition on ρ is known as the condition of contraction mapping for the equation (12) and similarly, we can calculate the condition of contraction mapping for the equations (13),(1314) and (15) as,

$$\rho_e \leq \left[\frac{\nu|\Gamma(\nu)|}{[\gamma+\mu+\pi-\beta p(r+\varpi)]}\right]^{1/\nu}, \tag{58}$$

$$\rho_i \leq \left[\frac{\nu|\Gamma(\nu)|}{[(r+\mu)]}\right]^{1/\nu}, \tag{59}$$

$$\rho_q \leq \left[\frac{\nu|\Gamma(\nu)|}{[\theta+\mu]}\right]^{1/\nu}. \tag{60}$$

Finally, we are successfully extract that the equations (34),(3435),(343536) and (37) are the condition of contraction mappings for (12),(1213),(121314) and (15) respectively. Hence, under the conditions (34), (35), (36) and (37) of self-mapping and the conditions (57),(5758),(575859),(57585960) of contraction mapping for the system of time-fractional differential equations (12),(1213),(121314),(12131415) we are satisfied to claim that there must exist a unique solution for each of the equation of a system of time-fractional differential equations in COVID-19 model [20].

6 Basic reproduction number

The basic reproduction number of an infection is the expected number of cases directly produced by one infection in a population in which all individuals are susceptible to infection. It is denoted by R_0. We will evaluate this using a next-generation matrix[25]. This value describes whether the infection will stop or spread uniformly into the country.

Conditions of R_0 are

–If $R_0 > 1$, then the infection will uniformly spread into the susceptible class (epidemic exist).
–If $R_0 < 1$, then the infection will stop out (epidemic not exist).
–If $R_0 = 1$, then the infection will spread constantly.

To find the reproductive number, take the following matrices,

$$f = \begin{pmatrix} \beta N s(e+i) \\ 0 \end{pmatrix}, \quad v = \begin{pmatrix} \pi e + (\mu+\gamma)e \\ -\pi e + \sigma i + \mu i \end{pmatrix}.$$

Differentiate the matrix f and v with respect to the variable e and i, and take $s = 1$ we have

$$\frac{\partial F}{\partial e} = \beta N, \quad \frac{\partial F}{\partial i} = \beta N, \quad \frac{\partial F}{\partial e} = 0, \quad \frac{\partial F}{\partial i} = 0.$$

and

$$\frac{\partial V}{\partial e} = \pi + \mu + \gamma, \quad \frac{\partial V}{\partial i} = 0, \quad \frac{\partial V}{\partial e} = -\pi, \quad \frac{\partial V}{\partial i} = \sigma + \mu.$$

The deduced matrices F and V are:

$$F = \begin{pmatrix} \beta N & \beta N \\ 0 & 0 \end{pmatrix}, \quad V = \begin{pmatrix} \pi+\mu+\gamma & 0 \\ -\pi & \sigma+\mu \end{pmatrix}.$$

We can easily calculate that

$$FV^{-1} = \begin{pmatrix} \frac{\beta N(\sigma+\mu+\pi)}{(\pi+\mu+\gamma)(\sigma+\mu)} & \frac{\beta N}{\sigma+\mu} \\ 0 & 0 \end{pmatrix},$$

We know that the characteristic eigenvalue equation for the matrix is $|(FV^{-1}) - \zeta I| = 0$. and we have the eigenvalues,

$$\zeta = 0, \quad \zeta = \frac{\beta N(\sigma+\mu+\pi)}{(\pi+\mu+\gamma)(\sigma+\mu)}.$$

Thus the reproductive number of the disease is

$$R_0 = \frac{\beta N(\sigma+\mu+\pi)}{(\pi+\mu+\gamma)(\sigma+\mu)}.$$

7 Equilibrium points

This section analyzes two types of equilibrium points in the system and calculates both points by considering the fractional derivative of the model as zero, simplifying the equation, and substituting the equations[26].

1.Disease-free Equilibrium (DFE).
2.Endemic equilibrium (EE).

7.1 Disease-free equilibrium point (DFEP)

This analysis is related to calculating the disease-free equilibrium points of the (COVID-19) model, we have to put the fractional order derivatives equal to zero in all the equations of the fractional version system of the COVID-19 model[27].

$$\begin{aligned}
0 &= \mu - \mu s - \beta N s(e+i),\\
0 &= \beta N d(e+i) - \pi e - (\mu+\gamma)e,\\
0 &= \pi e - \sigma i - \mu i,\\
0 &= \gamma e + \sigma i - \theta q - \mu q.
\end{aligned}$$

These equations give the virus-free equilibrium (DFE) point $(1,0,0,0)$.

7.2 Endemic equilibrium point (EE)

This subpart explores an endemic equilibrium point of the system of fractional differential equation of the COVID-19 model, for this purpose of the study we again take the system where the derivative of the system has vanished

$$0 = \mu - \mu s - \beta N s(e+i), \tag{61}$$
$$0 = \beta N d(e+i) - \pi e - (\mu+\gamma)e, \tag{62}$$
$$0 = \pi e - \sigma i - \mu i, \tag{63}$$
$$0 = \gamma e + \sigma i - \theta q - \mu q. \tag{64}$$

From (61) we have

$$i = \frac{\mu - \mu s}{\beta N s} - e,$$

$$i = \frac{\pi(\mu R_0 - \mu)}{\beta N(\pi+\sigma+\mu)}.$$

Consider the equation (62) and use the equation (63) we have

$$\beta N s\left(e + \frac{\pi e}{\sigma+\mu}\right) = \pi e + (\mu+\gamma)e,$$

$$s = \frac{e}{\left(\frac{\beta N(\sigma+\mu+\pi)}{(\pi+\mu+\gamma)(\sigma+\mu)}\right)} = \frac{e}{R_0}.$$

From (63) we get

$$i = \frac{\pi e}{\sigma+\mu}.$$

From (64) we get

$$q = \frac{\gamma e + \sigma i}{\theta+\mu},$$

$$q = \frac{i(\gamma(\sigma+\mu)+\sigma\pi)}{\pi(\theta+\mu)}.$$

Lemma 1(7.1). *Let $V(t) \in \mathbb{R}^+$ be a continuous function. Then, for any time $t \geq t_0$,*

$${}_0^c D_t^{\nu}\left[V(t) - V^* - V^* \ln\frac{V(t)}{V^*}\right] \leq \left(\frac{V-V^*}{V(t)}\right) {}_0^c D_t^{\nu} V(t)$$

$V^* \in \mathbb{R}^+$, for all $\nu \in (0,1)$.

8 Stability

In this section, we analyzed the Global stability at disease free equilibrium point (DFE) $C_0 = (s,e,i,q) = (1,0,0,0)$ for the system with the help of below given results.

Theorem 8.1 The underlying COVID-19 system (12)-(15) is globally asymptotically stable at $C_0 = (s,e,i,q) = (1,0,0,0)$ under $R_0 < 1$.

*Proof.*Let us consider the Lyapunov function for a given differential system.

$$U : G \to \mathbb{R},$$

U must be less then 0 so, we can say that the system is stable at DFE point. and

$$U = s+e+i+q \quad \forall (s,e,i,q) \in G.$$

by using c_0,

$$U = s - s^0 \ln s + e + i + q,$$

applying lemma (7.1)

$${}_0^c D_t^\nu U(t) \leq {}_0^c D_t^\nu s(t) - \frac{s^0}{s} {}_0^c D_t^\nu s(t) + {}_0^c D_t^\nu e(t) + {}_0^c D_t^\nu i(t) + {}_0^c D_t^\nu q(t),$$

$${}_0^c D_t^\nu U(t) \leq \left(1 - \frac{s^0}{s}\right) {}_0^c D_t^\nu s(t) + {}_0^c D_t^\nu e(t) + {}_0^c D_t^\nu i(t) + {}_0^c D_t^\nu q(t).$$

Put the value of derivatives:

$${}_0^c D_t^\nu U(t) \leq \left(\frac{s-s^0}{s}\right)[\mu - \mu s - \beta N s(e+i)] + \beta N s(e+i) - \pi e - (\mu+\gamma)e$$

$$+\pi e - \sigma i - \mu i + \gamma e + \sigma i - \theta q - \mu q.$$

Now as the above term ${}_0^c D_t^\nu s(t) = 0$,

$${}_0^c D_t^\nu U(t) \leq \left(\frac{s-s^0}{s}\right)\left[\mu s^0 + \beta N s^0(e+i) - \mu s - \beta N s(e+i)\right]$$

$$+\beta N s(e+i) - \mu e - \mu i - \theta q - \mu q,$$

$${}_0^c D_t^\nu U(t) \leq \left(\frac{s-s^0}{s}\right)\left[\mu(s^0-s) + \beta N(e+i)(s^0-s)\right] + \beta N s(e+i) - (\mu e+i) - \theta q - \mu q,$$

$${}_0^c D_t^\nu U(t) \leq -\left(\frac{(s-s^0)^2}{s}\right)[\mu + \beta N(e+i)] + (e+i)\mu\left(\frac{\beta N s}{\mu} - 1\right) - \theta q - \mu q,$$

as we know that $R_0 = \frac{\beta N s}{\mu}$

$${}_0^c D_t^\nu U(t) \leq -\left(\frac{(s-s^0)^2}{s}\right)[\mu + \beta N(e+i)] + (e+i)\mu(R_0 - 1) - \theta q - \mu q \leq 0,$$

if $R_0 < 0$ then we can say that

$${}_0^c D_t^\nu U(t) \leq 0.$$

hence proved.

theorem 8.2 The underlying COVID-19 model (12)-(15) is globally asymptotically stable at $c_0 = (s^*,e^*,i^*,q^*) = \left(\frac{e}{R_0}, sR_0, \frac{\pi e}{\sigma+\mu}, \frac{i(\gamma(\sigma+\mu)+\sigma\pi)}{\pi(\theta+\mu)}\right)$ under $R_0 > 1$.

*Proof.*define,

$$U^* = s - s^* \ln s + e - e^* \ln e + i - i^* \ln i + q - q^* \ln q,$$

using lemma (7.1)

$${}_0^c D_t^\nu U^*(t) \leq {}_0^c D_t^\nu s(t) - \frac{s^*}{s} {}_0^c D_t^\nu s(t) + {}_0^c D_t^\nu e(t) - \frac{e^*}{e} {}_0^c D_t^\nu e(t) + {}_0^c D_t^\nu i(t) - \frac{i^*}{i} {}_0^c D_t^\nu i(t)$$

$$+ {}_0^c D_t^\nu q(t) - \frac{q^*}{q} {}_0^c D_t^\nu q(t),$$

$${}_0^c D_t^\nu U^*(t) \leq \left(1 - \frac{s^*}{s}\right) {}_0^c D_t^\nu s(t) + \left(1 - \frac{e^*}{e}\right) {}_0^c D_t^\nu e(t) + \left(-\frac{i^*}{i}\right) {}_0^c D_t^\nu i(t) + \left(1 - \frac{q^*}{q}\right) {}_0^c D_t^\nu q(t).$$

put the value of $[{}_0^c D_t^\nu s(t), {}_0^c D_t^\nu e(t), {}_0^c D_t^\nu i(t), {}_0^c D_t^\nu q(t)]$

$${}_0^c D_t^\nu U^*(t) \leq \left(\frac{s - s^*}{s}\right) [\mu - \mu s - \beta N s(e+i)] + \left(\frac{e - e^*}{e}\right) [\beta N s(e+i) - \pi e - (\mu + \gamma) e]$$

$$+ \left(\frac{i - i^*}{i}\right) [\pi e - \sigma i - \mu i] + \left(1 - \frac{q^*}{q}\right) [\gamma e + \sigma i - \theta q - \mu q],$$

$${}_0^c D_t^\nu U^*(t) \leq (s - s^*) \left[\frac{\mu}{s} - \mu - \beta N(e+i)\right] + (e - e^*) \left[\frac{\beta N s(e+i)}{e} - \pi - (\mu + \gamma)\right]$$

$$+ (i - i^*) \left[\frac{\pi e}{i} - \sigma - \mu\right] + (q - q^*) \left[\frac{\gamma e}{q} + \frac{\sigma i}{q} - \theta - \mu\right],$$

Now let

$${}_0^c D_t^\nu s(t) \leq {}_0^c D_t^\nu e(t) = {}_0^c D_t^\nu i(t) = {}_0^c D_t^\nu q(t) = 0,$$

implies that

$$\mu = \frac{\mu}{s^*} - \beta N(e+i), \tag{65}$$

$$\mu = \frac{\beta N s i}{e^*} + \beta N s - \pi - \gamma, \tag{66}$$

$$\mu = \frac{\pi}{i^*} e - \sigma, \tag{67}$$

$$\mu = \frac{\gamma e}{q^*} + \frac{\sigma i}{q^*} - \theta. \tag{68}$$

put (65)-(68) in the equation (??)

$${}_0^c D_t^\nu U^*(t) \leq (s - s^*) \left[\frac{\mu}{s} - \frac{\mu}{s^*} - \beta N(e+i) - \beta N(e+i)\right] + (e - e^*) \left[\frac{\beta N s(e+i)}{e} - \pi - \mu - \gamma\right]$$

$$+ (i - i^*) \left[\frac{\pi e}{i} - \sigma - \frac{\pi}{i^*} e + \sigma\right] + (q - q^*) \left[\frac{\gamma e}{q} - \frac{\sigma i}{q} - \theta - \frac{\gamma e}{q^*} + \frac{\sigma i}{q^*} + \theta\right],$$

$${}_0^c D_t^\nu U^*(t) \leq -(s - s^*)^2 \left[\frac{\mu}{s s^*} - 2\beta N(e+i)\right] - (e - e^*)^2 \left[\frac{\beta N s i}{e e^*}\right]$$

$$-(i - i^*)^2 \left[\frac{\pi e}{i i^*}\right] - (q - q^*)^2 \left[\frac{\gamma e - \sigma i}{q q^*}\right],$$

$${}_0^c D_t^\nu U^*(t) \leq 0$$

hence proved.

9 Finite difference numerical scheme

In this important section, we evaluate the GL-NSFD scheme for the fractional version system of the fractional-order differential equation of a modified SEIQR mathematical model for COVID-19[29].

$$
\begin{aligned}
{}_0^cD_t^{\nu} s(t)\big|_{t=t_n} &= \Lambda_n - \mu s(t)_{n+1} - \beta(N)_n s(t)_{n+1}(e(t)_n + i(t)_n),\\
{}_0^cD_t^{\nu} e(t)\big|_{t=t_n} &= \beta(N)_n s(t)_{n+1}(e(t)_{n+1} + i(t)_n) - \pi e(t)_{n+1} - (\mu+\gamma)e(t)_n,\\
{}_0^cD_t^{\nu} i(t)\big|_{t=t_n} &= \pi e(t)_{n+1} - \sigma i(t)_{N+1} - \mu i(t)_{n+1},\\
{}_0^cD_t^{\nu} q(t)\big|_{t=t_n} &= \gamma e(t)_{n+1} + \sigma i(t)_{n+1} - \theta q(t)_{n+1} - \mu q(t)_{n+1}.\\
{}_0^cD_t^{\nu} r(t)\big|_{t=t_n} &= \theta q(t)_{n+1} - \mu r(t)_{n+1}.
\end{aligned}
$$

The non standard difference approximation of Caputo operator operators given by Grunwald-Letnikov approach (G.L.Approach) for detail. We consider,

$$
{}^{(c^0)}D_t^{\nu} s(t) = \Lambda_n - \mu s(t)_{n+1} - \beta(N)_n s(t)_{n+1}(e(t)_n + i(t)_n),
$$

Now,

$$
c_0D_t^{\alpha} = \frac{1}{\phi(h)^{\alpha}}\left[s_{n+1} - \sum_{\nu=1}^{n+1} c_{\nu}^{\alpha} s_{n+1-\nu} - p_{n+1}^{\alpha} s_0 \right],
$$

So we have,

$$
\begin{aligned}
s_{n+1} - \sum_{\nu=1}^{n+1} c_{\nu}^{\alpha} s_{n+1-\nu} - p_{n+1}^{\alpha} s_0 &= \phi(h)^{\alpha}\Lambda_n - (\phi(h)^{\alpha})\mu s(t)_{n+1}\\
&\quad -(\phi(h)^{\alpha})\beta(N)_n s(t)_{n+1}(e(t)_n + i(t)_n),
\end{aligned}
$$

We get,

$$
s_{n+1} = \frac{\sum_{\nu=1}^{n+1} c_{\nu}^{\alpha} s_{n+1-\nu} - p_{n+1}^{\alpha} s_0 + \phi(h)^{\alpha}\Lambda_n}{1 + \phi(h)^{\alpha}\mu + \phi(h)^{\alpha}\beta(e_n + i_n)N},
$$

Similarly,

$$
\begin{aligned}
e_{n+1} &= \frac{\sum_{\nu=1}^{n+1} c_{\nu}^{\alpha} e_{n+1-\nu} - p_{n+1}^{\alpha} e_0 + \phi(h)^{\alpha}\beta s_{n+1}(e_n + i_n)}{1 + \phi(h)^{\alpha}\pi + \phi(h)^{\alpha}(\mu + r)},\\
i_{n+1} &= \frac{\sum_{\nu=1}^{n+1} c_{\nu}^{\alpha} i_{n+1-\nu} - p_{n+1}^{\alpha} i_0 + \phi(h)^{\alpha}\pi r_{n+1}}{1 + \phi(h)^{\alpha}\sigma + \phi(h)^{\alpha}\mu},\\
q_{n+1} &= \frac{\sum_{\nu=1}^{n+1} c_{\nu}^{\alpha} q_{n+1-\nu} - p_{n+1}^{\alpha} q_0 + \phi(h)^{\alpha}\gamma e_{n+1} + \phi(h)^{\alpha}\sigma i_{n+1}}{1 + \phi(h)^{\alpha}\theta + \phi(h)^{\alpha}\mu},\\
r_{n+1} &= \frac{\sum_{\nu=1}^{n+1} c_{\nu}^{\alpha} r_{n+1-\nu} - p_{n+1}^{\alpha} r_0}{1 + \phi(h)^{\alpha}\mu}.
\end{aligned}
$$

9.1 Positivity

Because the state variables in the model describe the subpopulations of the different compartments, the values of these variables must be positive. Therefore, the proposed scheme must preserve the positivity of numerical solutions. The same is confirmed by the following results:

theorem 9.1 Suppose that $s_0 \geq 0, e_0 \geq 0, i_0 \geq 0, q_0 \geq 0, r_0 \geq 0$ moreover, all the parameters involved in the model are positive then $s_n \geq 0, e_n \geq 0, i_n \geq 0, q_n \geq 0, r_n \geq 0, \forall n \in \{0,1,2,3,\ldots\}$.

*Proof.*Consider,

$$
s_{n+1} = \frac{\sum_{\nu=1}^{n+1} c_{\nu}^{\alpha} s_{n+1-\nu} - p_{n+1}^{\alpha} s_0 + \phi(h)^{\alpha}\Lambda_n}{1 + \phi(h)^{\alpha}\mu + \phi(h)^{\alpha}\beta(e_n + i_n)N},
$$

We can observe the positivity of the GL-NSFD Scheme by applying different values of n. Now for $n=0$ we have,

$$s_1 = \frac{\sum_{\nu=1}^{1} c_\nu^\alpha s_{1-\nu} - p_1^\alpha s_0 + \phi(h)^\alpha \Lambda_0}{1+\phi(h)^\alpha \mu + \phi(h)^\alpha \beta (e_0+i_0)N} > 0,$$

For $n=1$

$$s_2 = \frac{\sum_{\nu=1}^{2} c_\nu^\alpha s_{2-\nu} - p_2^\alpha s_0 + \phi(h)^\alpha \Lambda_1}{1+\phi(h)^\alpha \mu + \phi(h)^\alpha \beta (e_1+i_1)N} > 0,$$

For $n=2$

$$s_3 = \frac{\sum_{\nu=1}^{3} c_\nu^\alpha s_{3-\nu} - p_3^\alpha s_0 + \phi(h)^\alpha \Lambda_2}{1+\phi(h)^\alpha \mu + \phi(h)^\alpha \beta (e_2+i_2)N} > 0,$$

As we continue the process to touch the highest value of n we observe that,

$$s_{n+1} = \frac{\sum_{\nu=1}^{n+1} c_\nu^\alpha s_{n+1-\nu} - p_{n+1}^\alpha s_0 + \phi(h)^\alpha \Lambda_n}{1+\phi(h)^\alpha \mu + \phi(h)^\alpha \beta (e_n+i_n)N} > 0,$$

Where $s_j, e_j, i_j, q_j, r_j, \forall j = 1,2,3,\ldots,n$ and $c_j^\alpha, r_j, \phi(h)^\alpha \Lambda, \mu, \beta, N \forall j = 1,2,3,\ldots,n$ are always positive at every time. Now by carrying the same process for remaining equations we can observe that.

$$e_{n+1} = \frac{\sum_{\nu=1}^{n+1} c_\nu^\alpha e_{n+1-\nu} - p_{n+1}^\alpha e_0 + \phi(h)^\alpha \beta s_{n+1}(e_n+i_n)}{1+\phi(h)^\alpha \pi + \phi(h)^\alpha (\mu+r)} > 0,$$

$$i_{n+1} = \frac{\sum_{\nu=1}^{n+1} c_\nu^\alpha i_{n+1-\nu} - p_{n+1}^\alpha i_0 + \phi(h)^\alpha \pi r_{n+1}}{1+\phi(h)^\alpha \sigma + \phi(h)^\alpha \mu} > 0,$$

$$q_{n+1} = \frac{\sum_{\nu=1}^{n+1} c_\nu^\alpha q_{n+1-\nu} - p_{n+1}^\alpha q_0 + \phi(h)^\alpha \gamma e_{n+1} + \phi(h)^\alpha \sigma i_{n+1}}{1+\phi(h)^\alpha \theta + \phi(h)^\alpha \mu} > 0,$$

$$r_{n+1} = \frac{\sum_{\nu=1}^{n+1} c_\nu^\alpha r_{n+1-\nu} - p_{n+1}^\alpha r_0}{1+\phi(h)^\alpha \mu} > 0.$$

9.2 Boundedness

Since, all the state variables in the model describe the sizes of the populaces, so they can not be infinite at any time t. Because, infinite population of any compartment is physically meaningless. Therefore, the population of any compartment or the sum of populations of all the compartments must be finite and positively bounded. To this end, the following results were established.

theorem 9.2 Suppose that $s_0+e_0+i_0+q_0+r_0=1$, $(\phi(h))^\alpha \geq 0$ for $\alpha \in (0,1)$ and all the control parameters are positive then s_n, e_n, i_n, q_n, r_n are bounded $\forall n = 1,2,3,\ldots,n$ where $D_n = \sum_\nu^n c_\nu^\alpha (s_{n-\nu}+e_{n-\nu}+i_{n-\nu}+q_{n-\nu}+r_{n-\nu}) + p_n + \phi(h)^\alpha \mu + \phi(h)^\alpha \gamma e_n$.

Proof. As,

$$s_{n+1} = \frac{\sum_{\nu=1}^{n+1} c_\nu^\alpha s_{n+1-\nu} - p_{n+1}^\alpha s_0 + \phi(h)^\alpha \Lambda_n}{1+\phi(h)^\alpha \mu + \phi(h)^\alpha \beta (e_n+i_n)N},$$

$$e_{n+1} = \frac{\sum_{\nu=1}^{n+1} c_\nu^\alpha e_{n+1-\nu} - p_{n+1}^\alpha e_0 + \phi(h)^\alpha \beta s_{n+1}(e_n+i_n)}{1+\phi(h)^\alpha \pi + \phi(h)^\alpha (\mu+r)},$$

$$i_{n+1} = \frac{\sum_{\nu=1}^{n+1} c_\nu^\alpha i_{n+1-\nu} - p_{n+1}^\alpha i_0 + \phi(h)^\alpha \pi r_{n+1}}{1+\phi(h)^\alpha \sigma + \phi(h)^\alpha \mu},$$

$$q_{n+1} = \frac{\sum_{\nu=1}^{n+1} c_\nu^\alpha q_{n+1-\nu} - p_{n+1}^\alpha q_0 + \phi(h)^\alpha \gamma e_{n+1} + \phi(h)^\alpha \sigma i_{n+1}}{1+\phi(h)^\alpha \theta + \phi(h)^\alpha \mu},$$

$$r_{n+1} = \frac{\sum_{\nu=1}^{n+1} c_\nu^\alpha r_{n+1-\nu} - p_{n+1}^\alpha r_0}{1+\phi(h)^\alpha \mu},$$

Implies that,

$$s_{n+1}[1+\phi(h)^{\alpha}\mu+\phi(h)^{\alpha}\beta(e_n+i_n)N]=\sum_{v=1}^{n+1}c_v^{\alpha}s_{n+1-v}-p_{n+1}^{\alpha}s_0+\phi(h)^{\alpha}\Lambda_n,$$

$$e_{n+1}[1+\phi(h)^{\alpha}\pi+\phi(h)^{\alpha}(\mu+r)]=\sum_{v=1}^{n+1}c_v^{\alpha}e_{n+1-v}-p_{n+1}^{\alpha}e_0+\phi(h)^{\alpha}\beta s_{n+1}(e_n+i_n),$$

$$i_{n+1}[1+\phi(h)^{\alpha}\sigma+\phi(h)^{\alpha}\mu]=\sum_{v=1}^{n+1}c_v^{\alpha}i_{n+1-v}-p_{n+1}^{\alpha}i_0+\phi(h)^{\alpha}\pi r_{n+1},$$

$$q_{n+1}[1+\phi(h)^{\alpha}\theta+\phi(h)^{\alpha}\mu]=\sum_{v=1}^{n+1}c_v^{\alpha}q_{n+1-v}-p_{n+1}^{\alpha}q_0+\phi(h)^{\alpha}\gamma e_{n+1}+\phi(h)^{\alpha}\sigma i_{n+1},$$

$$r_{n+1}[1+\phi(h)^{\alpha}\mu]=\sum_{v=1}^{n+1}c_v^{\alpha}r_{n+1-v}-p_{n+1}^{\alpha}r_0.$$

Now we are summing all the equations as we taking the sum of Left hand sides in left hand sides and right hand sides in right hand sides,

$$s_{n+1}[1+\phi(h)^{\alpha}\mu]+e_{n+1}[1+\phi(h)^{\alpha}(\mu+r)]+i_{n+1}[1+\phi(h)^{\alpha}\mu]$$
$$+q_{n+1}[1+\phi(h)^{\alpha}\theta+\phi(h)^{\alpha}\mu]+r_{n+1}[1+\phi(h)^{\alpha}\mu]$$
$$=\sum_{v=1}^{n+1}c_v^{\alpha}s_{n+1-v}+e_{n+1-v}+i_{n+1-v}+r_{n+1-v}+r_{n+1}+\phi(h)^{\alpha}\mu+\phi(h)^{\alpha}\gamma e_{n+1}$$

Taking $n=0$ we will get,

$$s_1[1+\phi(h)^{\alpha}\mu]+e_1[1+\phi(h)^{\alpha}(\mu+r)]+i_1[1+\phi(h)^{\alpha}\mu]$$
$$+q_1[1+\phi(h)^{\alpha}\theta+\phi(h)^{\alpha}\mu]+r_1[1+\phi(h)^{\alpha}\mu]$$
$$=\sum_{v=1}^{1}c_v^{\alpha}s_{1-v}+e_{1-v}+i_{1-v}+r_{1-v}+p_1+\phi(h)^{\alpha}\mu+\phi(h)^{\alpha}\gamma e_1,$$

$$[1+\phi(h)^{\alpha}\mu][s_1+e_1\phi(h)^{\alpha}r)+i_1+q_1\phi(h)^{\alpha}\theta+r_1]$$
$$=c_1^{\alpha}(s_0+e_0+i_0+r_0)+p_1^{\alpha}+\phi(h)^{\alpha}\mu+\phi(h)^{\alpha}\gamma e_1,$$

Since, $(s_0+e_0+i_0+q_0)=1$. So,

$$[1+\phi(h)^{\alpha}\mu][s_1+e_1\phi(h)^{\alpha}r)+i_1+q_1\phi(h)^{\alpha}\theta+r_1]$$
$$=c_1^{\alpha}+p_1^{\alpha}+\phi(h)^{\alpha}\mu+\phi(h)^{\alpha}\gamma e_1,$$
$$s_1[1+\phi(h)^{\alpha}\mu]+e_1[1+\phi(h)^{\alpha}(\mu+r)]+i_1[1+\phi(h)^{\alpha}\mu]$$
$$+q_1[1+\phi(h)^{\alpha}\theta+\phi(h)^{\alpha}\mu]+r_1[1+\phi(h)^{\alpha}\mu]$$
$$=\left(\alpha+\frac{1}{\Gamma(1-\alpha)}+\phi(h)^{\alpha}(\Lambda+pe_1)\right).$$

since,

$$\left[\alpha+\frac{1}{\Gamma(1-\alpha)}+\phi(h)^{\alpha}(\mu+pe_1)\right]=D_1.$$

So that,

$$s_1[1+\phi(h)^{\alpha}\mu]\leq D_1,$$

Or,

$$s_1\leq\frac{D_1}{[1+\phi(h)^{\alpha}\mu]},$$

Similarly we have,

$$e_1 \leq \frac{D_1}{[1+\phi(h)^\alpha(\mu+r)]}, \quad i_1 \leq \frac{D_1}{[1+\phi(h)^\alpha\mu]},$$
$$q_1 \leq \frac{D_1}{[1+\phi(h)^\alpha\theta+\phi(h)^\alpha\mu]}, \quad r_1 \leq \frac{D_1}{[1+\phi(h)^\alpha\mu]}.$$

Which shows that $s_1 \leq D_1, e_1 \leq D_1, i_1 \leq D_1, q_1 \leq D_1$ and $r_1 \leq D_1$. Next, we are taking $n = 1$,

$$s_2[1+\phi(h)^\alpha\mu]+e_2[1+\phi(h)^\alpha(\mu+r)]+i_2[1+\phi(h)^\alpha\mu]$$
$$+q_2[1+\phi(h)^\alpha\theta+\phi(h)^\alpha\mu]+r_2[1+\phi(h)^\alpha\mu]$$
$$=\sum_{v=1}^{2} c_v^\alpha s_{2-v}+e_{2-v}+i_{2-v}+r_{2-v}+p_2+\phi(h)^\alpha\mu+\phi(h)^\alpha\gamma e_2,$$

Subsequently, we reach at the following expression,

$$s_2 \leq \frac{D_2}{[1+\phi(h)^\alpha\mu]}$$
$$e_2 \leq \frac{D_2}{[1+\phi(h)^\alpha(\mu+r)]}$$
$$i_2 \leq \frac{D_2}{[1+\phi(h)^\alpha\mu]}$$
$$q_2 \leq \frac{D_2}{[1+\phi(h)^\alpha\theta+\phi(h)^\alpha\mu]}$$
$$r_2 \leq \frac{D_2}{[1+\phi(h)^\alpha\mu]}$$

Where,

$$D_2 = c_1^\alpha(5D_1)+c_2^\alpha+p_2+\phi(h)^\alpha\mu+\phi(h)^\alpha\gamma e_2$$

As we continue the process we will approach the following results for $n \in \mathbb{Z}^+$

$$s_{n+1} \leq \frac{D_{n+1}}{[1+\phi(h)^\alpha\mu]}$$
$$e_{n+1} \leq \frac{D_{n+1}}{[1+\phi(h)^\alpha(\mu+r)]}$$
$$i_{n+1} \leq \frac{D_{n+1}}{[1+\phi(h)^\alpha\mu]}$$
$$q_{n+1} \leq \frac{D_{n+1}}{[1+\phi(h)^\alpha\theta+\phi(h)^\alpha\mu]}$$
$$r_{n+1} \leq \frac{D_{n+1}}{[1+\phi(h)^\alpha\mu]}$$

Which finally Shows that,

$$s_{n+1} < D_{n+1}, \quad e_{n+1} < D_{n+1}, \quad i_{n+1} < D_{n+1}, \quad q_{n+1} < D_{n+1}, \quad r_{n+1} < D_{n+1},$$

where $D_n = \sum_v^n c_v^\alpha(s_{n-v}+e_{n-v}+i_{n-v}+q_{n-v}+r_{n-v})+p_n+\phi(h)^\alpha\mu+\phi(h)^\alpha\gamma e_n$. Hence proved.

10 Numerical Example and Simulations

This section presents a numerical example and simulations of the disease [39,40]. The set of parametric values for the simulations at both steady states is given below:

Table 1: Values of the parameters

Parameters	For endemic point	For disease-free point
μ	0.5	0.5
β	0.9	0.5
π	0.085432	0.5
γ	0.00398	0.5
σ	0.2	0.5
N	1	0.5
τ	0.1	0.54

10.1 Virus Free State

Plots of various graphs are shown for four distinct orders of the fractional derivative. The graphs clearly show that each curve converges to a precise steady state or disease-free equilibrium point. In addition, the rate of convergence varied depending on the values. The graphs show that the pace of convergence slows for smaller values, and the likelihood of convergence increases with increasing value. The equivalent outcome of the convergence is directly proportional to the value.

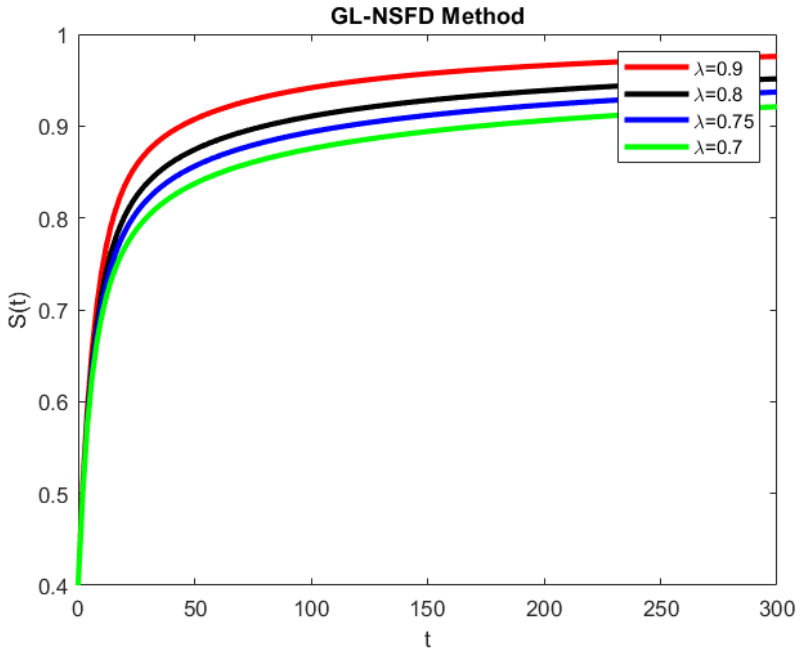

Fig. 1: Graphical solution of susceptible populace with different values of λ

Additionally, each graph follows a distinct path to reach the equilibrium point that is also linked to the fractional order parameter. Table 1 lists the values of each parameter that was used in the model. The behavior of those who are predisposed to contracting hepatitis B virus is depicted in Figure 1 for various values.

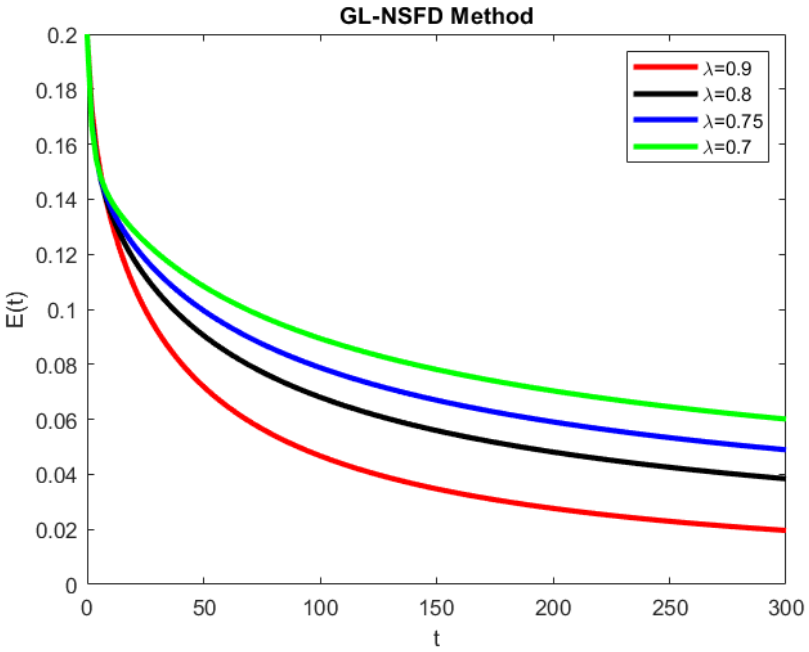

Fig. 2: Graphical solution of latent populace with different values of λ

The behavior of a function of people exposed to the coronavirus is depicted in Figure 2 for various parameter values. The derivatives of the functions are non-integers. The graph in Figure 1 demonstrates that for all specified values of the fractional-order parameter, all the sketched curves converged.

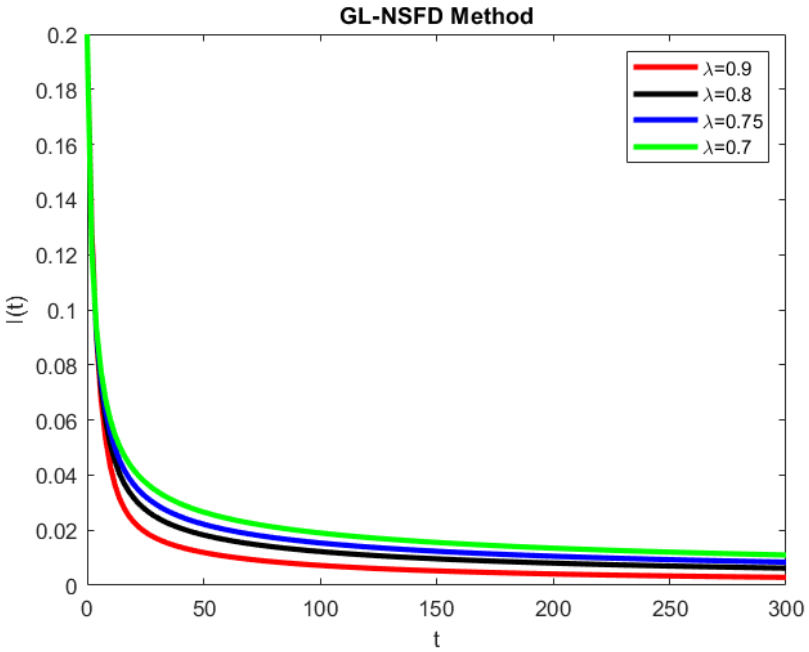

Fig. 3: Graphical solution of infected populace with different values of λ

Figure 3 depicts the behavior of people infected with the coronavirus. Infection with various parameter values. The curved lines converge on a condition free of sickness.

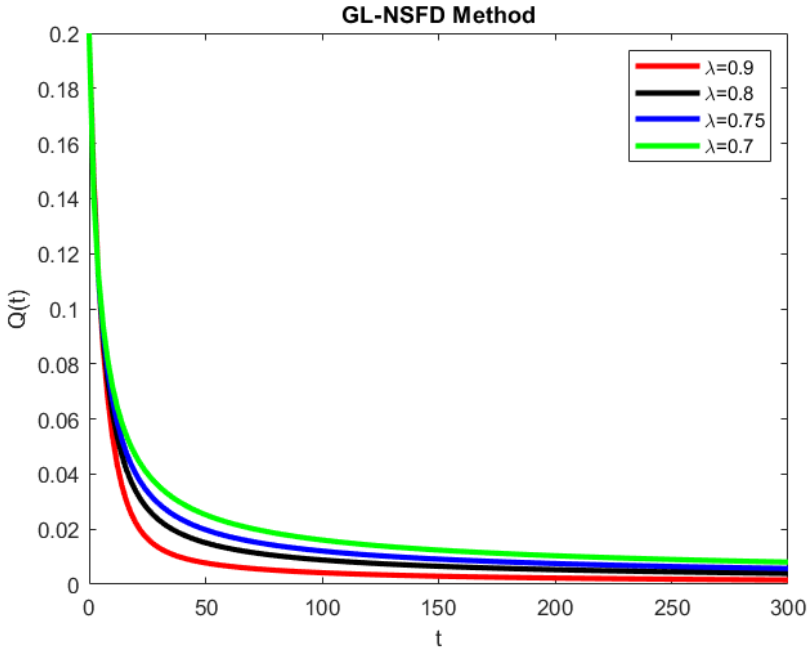

Fig. 4: Graphical solution of recovered populace with different values of λ

The graphs in Fig. 4 show the behavior of the carrier compartment. The various graphs illustrate how the carrier population changes over time. The line curve converges to the actual steady state or steady state in which there are no diseases. The graph shows the fractional-order parameters.

10.2 Virus Existence State

Figure 5 illustrates the dynamic behavior of the exposed compartment. The graphs show the fractional ordering parameters used. All curved lines reach the fixed point, but the rate at which they converge varies depending on the values of the parameter for fractional order. The values of the four separate graphs were plotted against the fractional order parameter of the model.

Behavior of individuals susceptible to the coronavirus. The winding drawing combined to the exact infection-free steady state by the altered values of fractional order λ.

The behavior of people who recovered from coronavirus disease. The winding drawing combined the exact infection-free steady state by every other value of fractional order λ. The graphs also show that every bent line joins the true stable state with a partial joining rate. It is also a reminder that the fractional order λ controls the path and hurry of the graph.

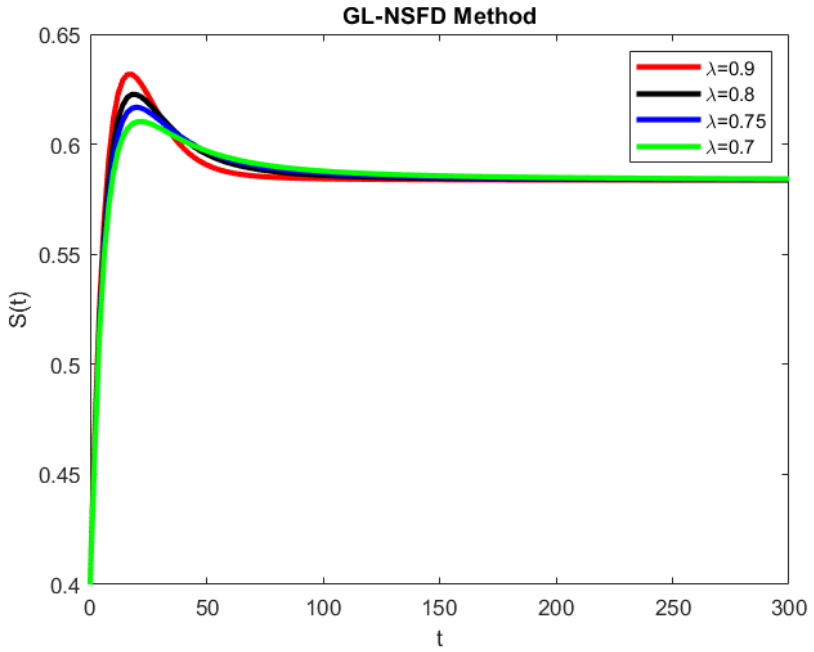

Fig. 5: Graphical solution of susceptible populace with different values of λ

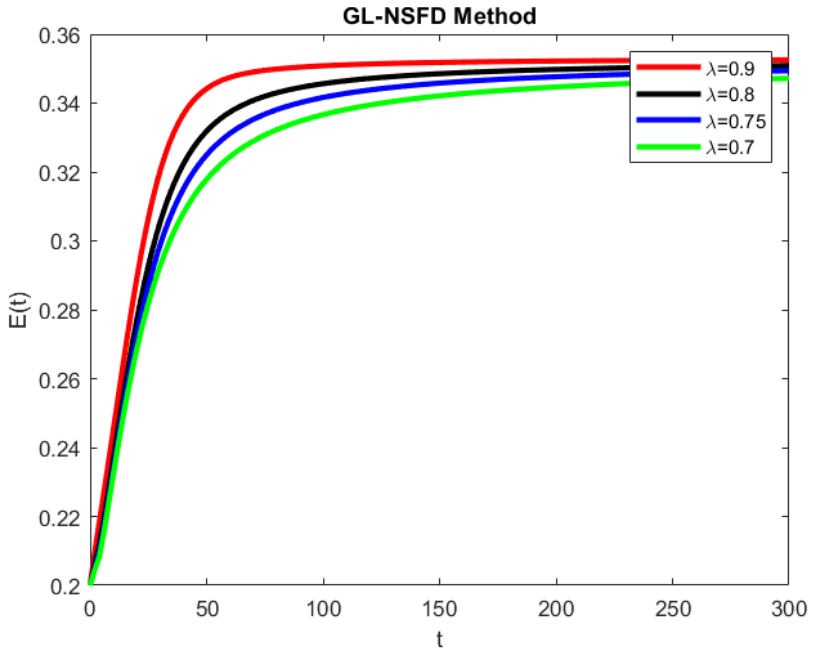

Fig. 6: Graphical solution of latent populace with different values of λ

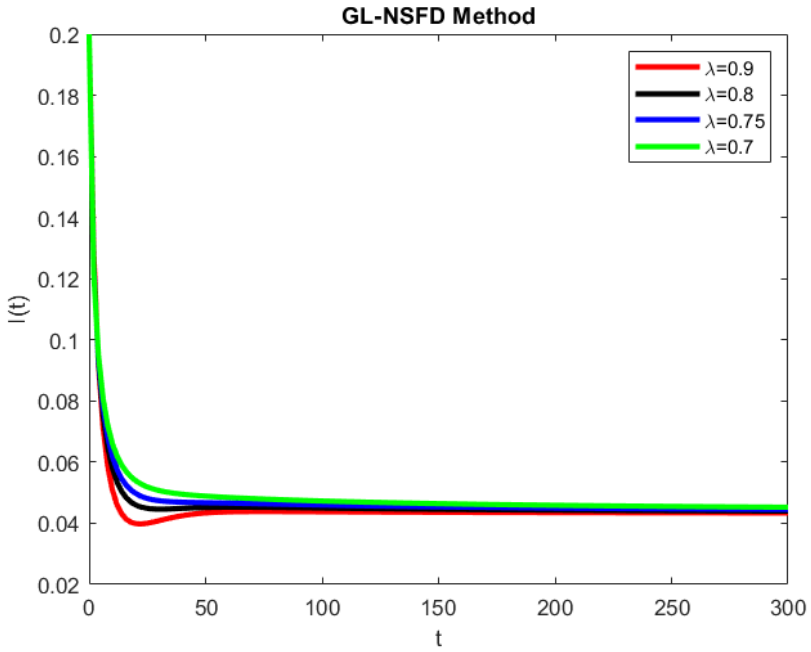

Fig. 7: Graphical solution of infected populace with different values of λ

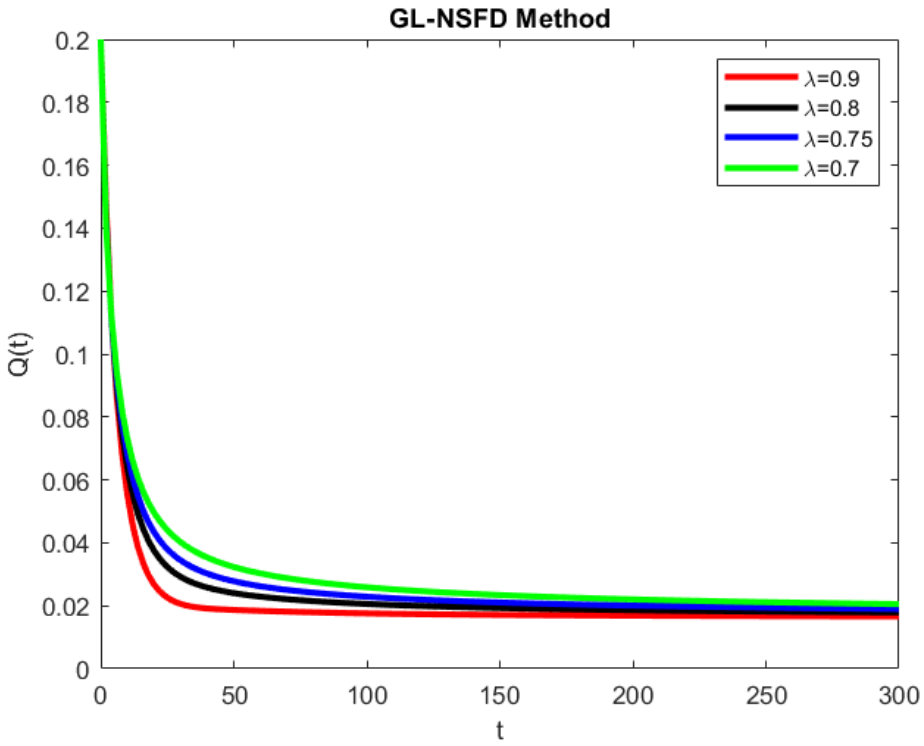

Fig. 8: Graphical solution of recovered populace with different values of λ

11 Conclusion

This article discusses the coronavirus model given in [30]. Based on the epidemic disease of COVID-19 in mainland China, we developed data-driven SEIQR models to investigate with a new modified fractional version of the Caputo fractional COVID-19 model. We analyzed the existence and uniqueness of the solution by applying the Banach fixed point theorem, contraction mapping principle, and Schauder theorem, including the Arzela-Ascoli theorem for relative compactness in the sequences. Utilizing the Lipschitz condition on the function value of two different points to confirm the unique solution of the epidemic dynamics model also represented the COVID-19 model in the system of fractional order differential equation and evaluated the GL-NSFD Scheme of the descriptive fractional version of the model.

Acknowledgments

The authors would like to use this opportunity to extend their heartfelt appreciation to everyone who has helped bring this research endeavor and article publishing to a successful conclusion. Their assistance and motivation were beneficial throughout the process. We express our gratitude to the invaluable resources and facilities offered by Siirt University Art and Science Faculty Department of Mathematics, TR-56100 Siirt, Turkey, and INTI International University, Malaysia, which were essential for the successful implementation of this research project.

References

[1] Ciotti, M., Ciccozzi, M., Terrinoni, A., Jiang, W. C., Wang, C. B., & Bernardini, S. (2020). The COVID-19 pandemic. *Critical Reviews in Clinical Laboratory Sciences*, 57(6), 365-388.
[2] Velavan, T. P., & Meyer, C. G. (2020). The COVID-19 epidemic. *Tropical Medicine & International Health*, 25(3), 278.
[3] Adiga, A., Dubhashi, D., Lewis, B., Marathe, M., Venkatramanan, S., & Vullikanti, A. (2020). Mathematical models for COVID-19 pandemic: A comparative analysis. *Journal of the Indian Institute of Science*, 100(4), 793-807.
[4] Noreen, N., Dil, S., Niazi, S., Naveed, I., Khan, N., Khan, F., . . . , & Kumar, D. (2020). COVID-19 pandemic in Pakistan: Limitations and gaps. *Global Biosecurity*, 2(1).
[5] Ilyas, N., Azuine, R. E., & Tamiz, A. (2020). COVID-19 pandemic in Pakistan. *International Journal of Translational Medical Research and Public Health*, 4(1), 37-49.
[6] Jebril, N. (2020). World Health Organization declared a pandemic public health menace: A systematic review of the coronavirus disease 2019 "COVID-19". *Available at SSRN 3566298*.
[7] Siche, R. (2020). What is the impact of COVID-19 disease on agriculture?. *Scientia Agropecuaria*, 11(1), 3-6.
[8] Balkhair, A. A. (2020). COVID-19 pandemic: A new chapter in the history of infectious diseases. *Oman Medical Journal*, 35(2), e123.
[9] Gopalan, H. S., & Misra, A. (2020). COVID-19 pandemic and challenges for socio-economic issues, healthcare and National Health Programs in India. *Diabetes & Metabolic Syndrome: Clinical Research & Reviews*, 14(5), 757-759.
[10] Khajanchi, S., Sarkar, K., & Mondal, J. (2020). Dynamics of the COVID-19 pandemic in India. *arXiv preprint arXiv:2005.06286*.
[11] Abdel-Gawad, H. I., & Abdel-Gawad, A. H. (2021). Discrete and continuum models of COVID-19 virus, formal solutions, stability and comparison with real data. *Mathematics and Computers in Simulation*, 190, 222-230.
[12] Baba, I. A., Yusuf, A., Nisar, K. S., Abdel-Aty, A. H., & Nofal, T. A. (2021). Mathematical model to assess the imposition of lockdown during COVID-19 pandemic. *Results in Physics*, 20, 103716.
[13] Velu, S. R., Ravi, V., & Tabianan, K. (2022). Predictive analytics of COVID-19 cases and tourist arrivals in ASEAN based on COVID-19 cases. *Health and Technology*, 12, 1237-1258.
[14] Owusu-Mensah, I., Akinyemi, L., Oduro, B., & Iyiola, O. S. (2020). A fractional order approach to modeling and simulations of the novel COVID-19. *Advances in Difference Equations*, 2020(1), 1-21.
[15] Iqbal, M. S., Ahmed, N., Akgül, A., Raza, A., Shahzad, M., Iqbal, Z., . . . , & Jarad, F. (2022). Analysis of the fractional diarrhea model with Mittag-Leffler kernel. *AIMS Mathematics*, 7(7), 13000-13018.
[16] Liu, C., Liu, L., Cao, J., Abdel-Aty, M. (2023) Intermittent Event-Triggered Optimal Leader-Following Consensus for Nonlinear Multi-Agent Systems Via Actor-Critic Algorithm, IEEE Transactions on Neural Networks and Learning Systems, 34(8), pp. 3992–4006 http://dx.doi.org/10.1109/TNNLS.2021.3122458
[17] Wang, Z., Cao, J., Lu, G., Abdel-Aty, M. (2020) Fixed-Time Passification Analysis of Interconnected Memristive Reaction-Diffusion Neural Networks, IEEE Transactions on Network Science and Engineering, 7(3), pp. 1814–1824, 8906166 http://dx.doi.org/10.1109/TNSE.2019.2954463
[18] Wang, Z., Cao, J., Cai, Z., Abdel-Aty, M. (2020) A novel Lyapunov theorem on finite/fixed-time stability of discontinuous impulsive systems, Chaos, 2020, 30(1), 013139 http://dx.doi.org/10.1063/1.5121246
[19] Abdel-Aty, M., Moya-Cessa, H. (2007) Sudden death and long-lived entanglement of two trapped ions, Physics Letters A, 369(5-6), pp. 372–376 http://dx.doi.org/10.1016/j.physleta.2007.05.003

[20] Abdalla, M.S., Abdel-Aty, M., Obada, A.-S.F. (2002) Degree of entanglement for anisotropic coupled oscillators interacting with a single atom, Journal of Optics B 4(6), pp. 396–401 http://dx.doi.org/10.1088/1464-4266/4/6/305
[21] Abdel-Aty, M. (2002) General formalism of interaction of a two-level atom with cavity field in arbitrary forms of nonlinearities, Physica A 313(3-4), pp. 471–487 http://dx.doi.org/10.1016/S0378-4371(02)00999-8
[22] Abdalla, M.S., Obada, A.-S.F., Abdel-Aty, M. (2005) Von Neumann entropy and phase distribution of two mode parametric amplifier interacting with a single atom, Annals of Physics, 318(2), pp. 266–285 http://dx.doi.org/10.1016/j.aop.2005.01.002
[23] Abdel-Aty, M., Abdel-Khalek, S., Obada, A.-S.F. (2000) Pancharatnam phase of two-mode optical fields with Kerr nonlinearity, Optical Review, 7(6), pp. 499–504 http://dx.doi.org/10.1007/s10043-000-0499-6
[24] Obada, A.-S.F., Abdel-Hafez, A.M., Abdelaty, M. (1998) Phase properties of a Jaynes-Cummings model with Stark shift and Kerr medium, European Physical Journal D, 3(3), pp. 289–294 http://dx.doi.org/10.1007/s100530050176
[25] Karaagac, B., & Owolabi, K. M. (2021). Numerical analysis of polio model: A mathematical approach to epidemiological model using derivative with Mittag-Leffler kernel. *Mathematical Methods in the Applied Sciences*.
[26] Erturk, V. S., & Kumar, P. (2020). Solution of a COVID-19 model via new generalized Caputo-type fractional derivatives. *Chaos, Solitons & Fractals*, 139, 110280.
[27] Logeswari, K., Ravichandran, C., & Nisar, K. S. (2020). Mathematical model for spreading of COVID-19 virus with the Mittag-Leffler kernel. *Numerical Methods for Partial Differential Equations*.
[28] Ahmad, S., Ullah, A., Al-Mdallal, Q. M., Khan, H., Shah, K., & Khan, A. (2020). Fractional order mathematical modeling of COVID-19 transmission. *Chaos, Solitons & Fractals*, 139, 110256.
[29] Tuan, N. H., Mohammadi, H., & Rezapour, S. (2020). A mathematical model for COVID-19 transmission by using the Caputo fractional derivative. *Chaos, Solitons & Fractals*, 140, 110107.
[30] Zhang, Y., Jiang, B., Yuan, J., & Tao, Y. (2020). The impact of social distancing and epicenter lockdown on the COVID-19 epidemic in mainland China: A data-driven SEIQR model study. *medRxiv*, 2020-03.
[31] Iqbal, M. S., Ahmed, N., Akgül, A., Raza, A., Shahzad, M., Iqbal, Z., & Jarad, F. (2022). Analysis of the fractional diarrhea model with Mittag-Leffler kernel. *AIMS Mathematics*, 7, 13000-13018.
[32] Babakhani, A., & Daftardar-Gejji, V. (2003). Existence of positive solutions of nonlinear fractional differential equations. *Journal of Mathematical Analysis and Applications*, 278(2), 434-442.
[33] Dietz, K. (1993). The estimation of the basic reproduction number for infectious diseases. *Statistical Methods in Medical Research*, 2(1), 23-41.
[34] Guerra, F. M., Bolotin, S., Lim, G., Heffernan, J., Deeks, S. L., Li, Y., & Crowcroft, N. S. (2017). The basic reproduction number (R0) of measles: A systematic review. *The Lancet Infectious Diseases*, 17(12), e420-e428.
[35] Cui, Q., Xu, J., Zhang, Q., & Wang, K. (2014). An NSFD scheme for SIR epidemic models of childhood diseases with constant vaccination strategy. *Advances in Difference Equations*, 2014(1), 1-15.
[36] Zeb, A., Alzahrani, E., Erturk, V. S., & Zaman, G. (2020). Mathematical model for coronavirus disease 2019 (COVID-19) containing isolation class. *BioMed Research International*, 2020.
[37] Shah, K., Din, R. U., Deebani, W., Kumam, P., & Shah, Z. (2021). On nonlinear classical and fractional order dynamical system addressing COVID-19. *Results in Physics*, 24, 104069.
[38] Selvam, A. G. M., Alzabut, J., Vianny, D. A., Jacintha, M., & Yousef, F. B. (2021). Modeling and stability analysis of the spread of novel coronavirus disease COVID-19. *International Journal of Biomathematics*, 14(05), 2150035.
[39] Wintachai, P., & Prathom, K. (2021). Stability analysis of SEIR model related to efficiency of vaccines for COVID-19 situation. *Heliyon*, 7(4), e06812.
[40] Ahmed, N., Elsonbaty, A., Raza, A., Rafiq, M., & Adel, W. (2021). Numerical simulation and stability analysis of a novel reaction-diffusion COVID-19 model. *Nonlinear Dynamics*, 106, 1293-1310.